

## Mathematical Relationship between Ice Dendrite Size and Freezing Conditions in Tuna

Mi Jung Choi, Geun Pyo Hong, Dae Sik In, and Sang Gi Min\*

Animal Resources Research Center, Konkuk University, Seoul 143-701, Korea

**Abstract** The principal objective of this study was to investigate changes in ice dendrite size during the freezing of tuna, in order to formulate a mathematical model of ice dendrite size. The tuna was frozen via a uni-directional heat transfer. Thermogram analysis allowed us to determine the position of the freezing front versus time, which is referred to as the freezing front rate. The morphology of the ice dendrites was assessed via scanning electron microscopy after freeze-drying, and the retained pore size was measured as ice dendrites. We noted that the mean size of ice dendrites increased with the distance to the cooling plate; however, it decreased with reductions in the cooling rate and the cooling temperature. In addition, shorter durations of the freeze-drying process decreased the freezing front rate, resulting in a larger size of the ice dendrite pores that operate as water vapor sublimation channels. According to our results, we could derive a linear regression as an empirical mathematical model equation between the ice dendrite size and the inverse of the freezing front rate.

**Keywords:** ice dendrite size, freezing front rate, freeze-drying time, tuna

### Introduction

Freezing is a food preservation technology which ensures high food quality with long storage duration. In a variety of studies, researchers have controlled the operating conditions of freezing model systems in order to achieve an eating quality that is as close as possible to the original state (1-6). The final quality of a product and particularly the smooth texture or cooling sensation perceived by consumers when consuming frozen foods, are largely conditioned by the ice crystal distribution. These ice crystals contribute principally to the physical deterioration of food texture, depending on their size. In general, good quality control of frozen food texture depends on ensuring a large proportion of smaller ice crystals.

The first published studies on these subjects involved alloy solidification systems (2,7). It has been demonstrated, in the case of alloy uni-directional freezing, that the characteristic dendrite sizes were inversely proportional to the freezing front rate and to the temperature gradient in the solid material zone. In particular, for high solidification rates, these authors experimentally and theoretically demonstrated that the relationship between the characteristic mean size, noted as  $L$ , and often selected by certain authors Bomben and King (8) and Kochs *et al.* (9) to be the interdendritic distance, the solidification front rate  $R$ , and the thermal gradient  $G$  was of the type  $L \propto R^a \cdot G^b$ , in which  $a$  and  $b$  are constants from experimental studies conducted with model freezing systems. These constants can be obtained by mathematical regression between ice dendrite size and freezing rate. In the food domain, Bomben and King (8) previously proposed the following relationship in the case of apples:  $L \propto R^{-0.5} \cdot G^{-0.5}$ . For the freezing of starch

gels, Kochs *et al.* (9) confirmed the correlation proposed by Kurtz and Fisher (7) at high alloy solidification rates, namely  $L \propto R^{-0.25} \cdot G^{-0.5}$ . In the case of the uni-directional freezing of gelatin gels using a freezing apparatus, Woinet *et al.* (2) obtained the following relationships:  $L \propto R^{-1}$  or  $L \propto R^{-0.5} \cdot G^{-0.5}$ , depending on the freezing conditions.

Among commercial high quality frozen food products, tuna is one of the most common products requiring a fast freezing process immediately after fishing, and is consumed without cooking in many countries. Kang *et al.* (10) previously reported that the fishing dimension of the tuna fishery industry is approximately 165,000 tons globally. Furthermore, tuna is very significant from a nutritional point of view, in that it possesses abundant protein, low cholesterol, and high unsaturated fatty acid content. In most cases tuna is immediately frozen after fishing and stored at low temperature. Frozen tuna is distributed to consumer in frozen state and served after thawing in raw condition. So, it can be postulated that the freezing process of tuna is important parameter in order to estimate strongly its quality characteristics. For these reasons, we selected tuna as a real food model for this experiment, in order to characterize the influence of the freezing step on the size of ice dendrites. The principal objective of our experiment was to mathematically derive a model equation for the effects of cooling temperature on ice crystal size.

### Materials and Methods

**Materials** The samples were taken from akami tissue of yellowfin tuna, which was delivered by Dong Won Co., Ltd. (Seoul, Korea). Before delivery to experimental study the tuna was packed with crushed ice after spiking on head, evisceration and washing. The moisture content of the sample showed 72%.

**Determination of freezing kinetics** In order to freeze tuna uni-directionally, tuna was cut parallel to muscle fiber

\*Corresponding author: Tel: +82-2-450-3680; Fax: +82-2-455-1044

E-mail: foodeng301@paran.com

Received July 1, 2008; Revised January 22, 2009;

Accepted April 2, 2009

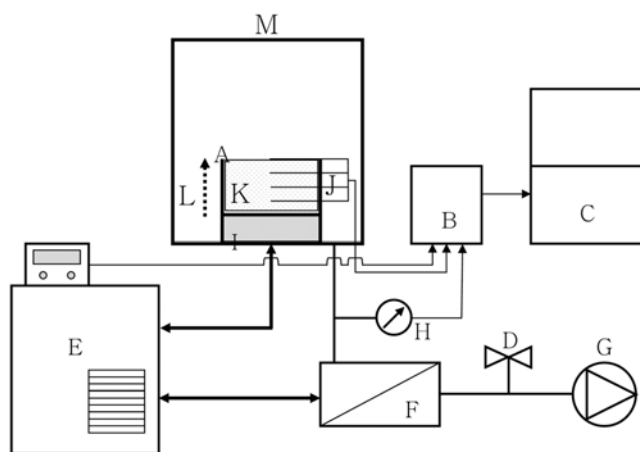


**Fig. 1. Schematic diagram of the experimental apparatus for freezing and freeze-drying.** A, freezing cell; B, data logger; C, acquisition device and computer; D, valve; E, cryostat and control unit; F, cold trap; G, vacuum pump; H, digital manometer; I, chopper plate (heat exchanger); J, thermocouples; K, sample (tuna); L, freezing direction; M, freeze dryer chamber.

in a shape ( $\phi 70 \times 20$  mm) and inserted in an acryl-glass cylinder with 20 mm height and 70 mm i.d. Four thermocouples (K-type) were introduced through the wall of the cylinder in order to record the temperatures at the following axial positions measured from the bottom: 5, 10, and 15 mm, and the final thermocouple was positioned on the top of the cylinder with its tip covered by tuna (Fig. 1). The cylinder wall was then insulated with styrofoam and the freezing cell was positioned in contact with a copper surface that could be maintained at  $-30$ ,  $-24$ ,  $-18$ , and  $-12$  °C, respectively, by external cryostat (Julabo FP 80; Julabo Labortechnik GmbH, Sellbach, Germany). In general, the chosen temperature range is available for food freezing industry. Temperatures were recorded by data acquisition system (MV-100; Yokogawa, Tokyo, Japan) every minute until the freezing process was complete.

**Freeze drying of frozen sample** The frozen cylindrical samples were subsequently freeze-dried in a lab-made freeze-dryer (consisting of a chamber, cold trap, vacuum pump, pressure gauge, and digital manometer) at a maximum pressure of 5 Pa (Fig. 1). The cold trap temperature was maintained at  $-80$  °C by external cryostat (E) (FW-80; Julabo) and the pressure level was measured with a digital manometer. Latent heat for sublimation was provided by heat conduction from the plates, which were maintained at  $25$  °C by cryostat (E). The end of freeze drying process was adjusted by measurement of sample temperature when the temperature of sample position 10 mm from the bottom reached at  $10$  °C. And then, the total freeze drying time depending on freezing temperature of  $-30$ ,  $-24$ ,  $-18$ , and  $-12$  °C was calculated.

**Morphology and analysis of ice dendrite size** The solid material after freeze drying was separated from the acryl-glass cylinder while maintaining its shape. The freeze-dried samples were vertically cut at half of each thermocouple height (2.5, 7.5, 12.5, and 17.5 mm) with a thin cutter. The

freeze-dried samples were then polished and sputter-coated (E-1010; Hitachi, Tokyo, Japan) with a thin gold layer (13 mA, 93.3 Pa, 70 sec). The samples were transferred under vacuum to a scanning electron microscope (Model S-3000N; Hitachi), where they were viewed and photographed. The size of the ice crystals was characterized by determining the pore size after freeze-drying the samples as Woinet *et al.* (2,3) and Faydi *et al.* (5) carried out similarly. The ice crystals, or more specifically the pores, were measured as diameter of ice dendrite using semi-automatic image analysis software (PPM; Arndt and Baumgartel GmbH, Germany) proposed by Min (17) for the first time. The software measured the size  $d$ , in accordance with a corresponding previous calibration. For each slide, approximately 100-300 crystals were measured, thus providing the crystal size distribution.

## Results and Discussion

Firstly, the transient temperature profile data were obtained, and analyzed them via regression fitting. From the thermal analysis profile, 2 overall heat transfer parameters could be deduced, the freezing front rate and the thermal gradients at the mean ice crystal size as a function of the cooling temperature.

### Experimental thermogram and regression fit analysis

During each freezing experiment, a thermogram was recorded. Figure 2 shows the temperature profile of tuna at a cooling temperature of  $-30$  °C. The thermogram analysis provided the exact freezing conditions, the position of the freezing front vs. time, and the freezing front temperature where a similar temperature profile was demonstrated by Woinet *et al.* (2, 3), Faydi *et al.* (5), and Pardo *et al.* (6).

Accordingly, the profile just above the freezing occurrence was not exactly a temperature for phase transition from water to ice, owing to the thermal inertia of the freezing cell generated by latent heat. A low thermal gradient existed through the sample (between 10 and 15 °C), so we adjusted for the initial temperature, designated  $T_{II}$ , or the mean temperature. The cooling temperature,  $T_I$ , was considered to be the copper plate temperature at the end of the acryl-glass cylinder freezing unit. As previously noted (2), the freezing front position was determined from the slope discontinuity of the thermograms, due to the fact that the thermocouple entered in a higher heat conductivity zone (freezing), thus resulting in a higher cooling rate. The freezing front temperature,  $T_m$ , was the thermocouple temperature at the slope breakdown level (indicated horizontal line in Fig. 2). According to our results, the initial freezing temperature of tuna was approximately  $-1.1$  °C, which is determined through the cross point of 2 linear fits for thermal line of precooling and freezing process at the 5 mm position. This value was similar at  $-1.2$  °C, as previously reported by Rahman and Sablandi (4). However, the slope discontinuity was difficult to identify at the position of 15 and 20 mm in Fig. 2 as Woinet *et al.* (2) found similar phenomena in freezing process of gelatin matrix.

For the regression fit of the thermal profiles in the tuna samples, the inverse sigmoid graph was obtained as shown in Fig. 2 (regression fit line). This equation of regression fit was expressed as exponential decay, as follows:

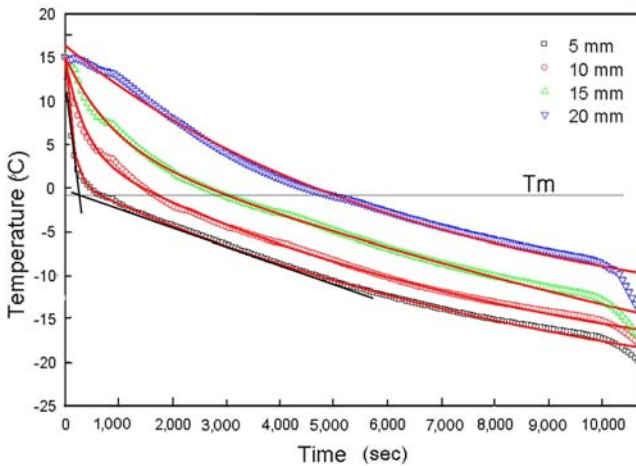


**Fig. 2.** Temperature profiles at different positions upon a typical uni-directional freezing process at  $-30^{\circ}\text{C}$  of cooling temperature and regression fit. Legend, axial positions measure from the bottom end of the sample. Solid horizontal line, the initial freezing temperature of sample.

**Table 1.** Parameters of exponential decay regression fit with  $y=y_0+A_1e^{-(x-x_0)/t_1}+A_2e^{-(x-x_0)/t_2}$  at different positions (cooling temperature:  $-30^{\circ}\text{C}$ ) from thermal experimental profiles,  $y_0$ ,  $x_0$ ,  $A_1$  ( $A_2$ ) and  $t_1$  ( $t_2$ ) represents offset, center, amplitude, and decay constant

Parameters	Position			
	5 mm	10 mm	15 mm	20 mm
$y_0$	-28.30	-24.71	-45.60	-21.11
$x_0$	0	0	0	0
$a_1$	14.40	10.30	9.62	17.77
$t_1$	126.80	370.49	851.60	4,838.71
$a_2$	29.23	28.92	51.05	19.70
$t_2$	9,979.86	8,701.90	21,797.76	14,564.16

$$T(x,t)=y_0+A_1e^{-\frac{(t-x_0)}{t_1}}+A_2e^{-\frac{(t-x_0)}{t_2}} \quad (1)$$

where  $y_0$  ( $^{\circ}\text{C}$ ),  $x_0$  (sec),  $A_1$  ( $^{\circ}\text{C}/\text{sec}$ ),  $A_2$  ( $^{\circ}\text{C}/\text{sec}$ ),  $t_1$  (sec), and  $t_2$  (sec) represent the offset, center, amplitude, and decay constant as fitting parameters, respectively. Table 1 shows their parameters at different positions at  $T_f=-30^{\circ}\text{C}$ . The value of  $t_1$  (decay constant) increases as the thermocouple moves away from the bottom. This indicates that the slope of the thermal profile lowers slowly due to the slower freezing rate. Some researchers have predicted the temperature fields and the freezing rate at the front position all along the freezing process in a model food system, using the Neumann analytical model (2-5). In our experiment, we simply calculated the temperature alteration via mathematical regression fitting.

**Freezing front position and time** As explained above, the movement of the freezing front can be determined using  $T_m$  (Fig. 2) as an indicator. In practice, the freezing time of each position could be calculated when each thermocouple detected the initial freezing temperature,  $-1.1^{\circ}\text{C}$  at any given instant. The initial freezing front position was plotted

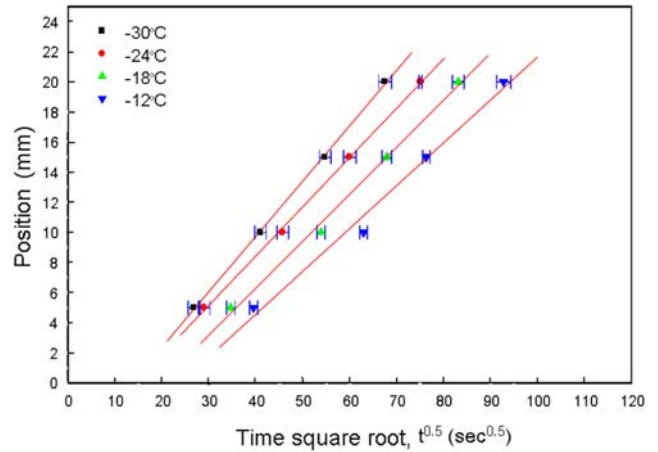


**Fig. 3.** Freezing time square ( $t^{0.5}$ ) as a function of the front location ( $s$ ) at different cooling temperature.

**Table 2.** Parameters  $a$  and  $b$  of the relationship between freezing front time,  $t^{0.5}$ , and the distance,  $s$ , by linear regression such like,  $s=a \cdot t^{0.5}+b$ ,  $a$ : slope,  $b$ : intercept, and  $r$ : correlation coefficient

Cooling temperature ( $^{\circ}\text{C}$ )	$a$ ( $\text{mm}/\text{sec}^{0.5}$ )	$b$ (mm)	$r$
-30	0.37	-4.98	0.9997
-24	0.33	-4.66	0.9995
-18	0.31	-6.19	0.9976
-12	0.28	-6.82	0.9932

as a function of the time square root in Fig. 3 on the different cooling temperatures. All of the results demonstrate a linear relationship between the freezing front position and the time square root, designated  $s$ , and  $t^{0.5}$ . Consequently, these plots could be interpreted by the following correlation in agreement with the results of Woinet *et al.* (2,3):

$$s=a\sqrt{t}+b \quad (2)$$

in which  $a$  and  $b$  represent the slope and the intercept. According to Table 2, the lower the cooling temperature was, the higher  $a$  value increased.

**Freezing front rate calculation** The freezing front rate, designated as  $R$ , was calculated by the time from the copper plate to each thermocouple when the ice front reached the axial position-thus the breakdown point of the slope as is demonstrated in the temperature profile shown in Fig. 2. Thus,  $R$  was calculated via derivation from the experimental curves of eq. 2 at different freezing front positions, and the results are shown in Fig. 4. As had been expected, we noted that, firstly for the distance to the cold wall, and secondly for a given position, the freezing front rate increased with decreasing cooling temperatures.

Furthermore, depending on the distance from the bottom (designated  $s$ ) the freezing rate became slower at the same cooling temperature. The study conducted by Woinet *et al.* (2,3) supports the notion that the freezing rate is related to the temperature gradient in the frozen zone, and also to the freezing front rate. It is worthy of note that the gradient between the sample temperature and the cooling

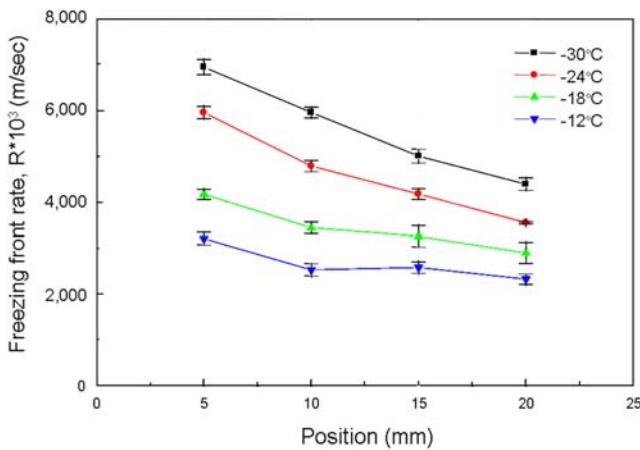


Fig. 4. Freezing front rate ( $R$ ) as a function of the front location ( $s$ ) at different cooling temperatures.

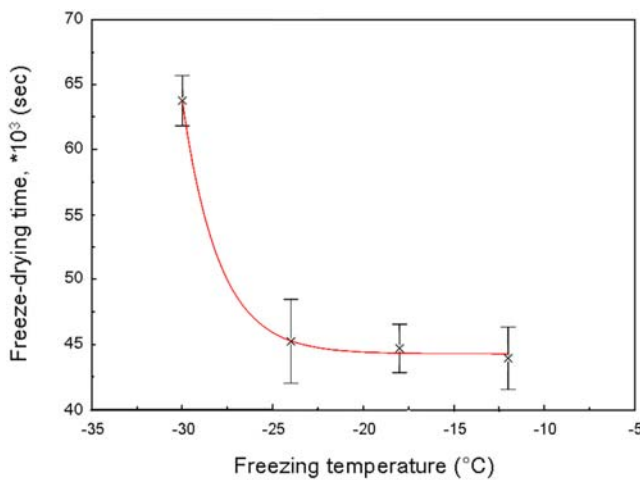


Fig. 5. Influence of cooling temperature on freeze-drying time in tuna.

temperature during freezing is related to the freezing time, that is, the rate of heat transfer.

**Freeze-drying time** The durations of freeze-drying time for the tuna were approximately 17 hr at  $T_f = -30^\circ\text{C}$  and 11.6 hr at  $T_f = -12^\circ\text{C}$ , thus indicating that fast freezing required more time for drying in order to complete the process of sublimation. In order to determine the relationship between the cooling temperature  $T_f$  and the freeze-drying time  $t_{fd}$ , we represented them mathematically by exponential decay regression, such that

$$t_{fd} = y_0 + A_1 e^{-\frac{(T_f - x_0)}{t_1}} \quad (3)$$

where  $y_0 = 43,817.2$ ,  $x_0 = -30$ ,  $A_1 = 20,707.8$ , and  $t_1 = 2.3$  represent the offset, center, amplitude, and decay constant, respectively.

As is shown in Fig. 5, increasing cooling temperature correlates with decreasing freeze-drying time. However, we noted that the freezing temperature of  $-24^\circ\text{C}$  may be a critical cooling temperature, below which no significant reduction of freeze drying time is achieved. Such phenomena

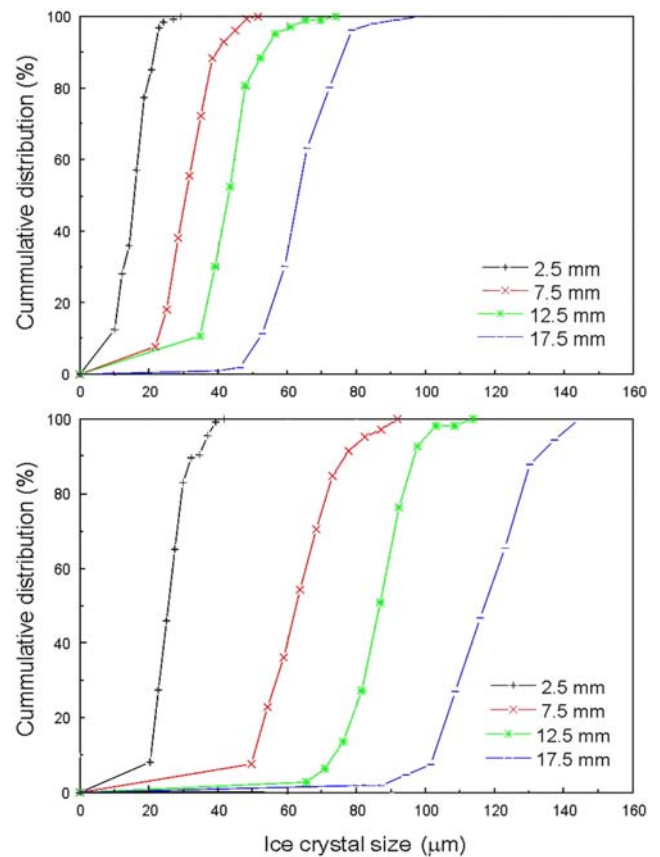


Fig. 6. Influence of the axial position at  $-30^\circ\text{C}$  (upper) and  $-12^\circ\text{C}$  (below) on evolution of ice crystal size.

show the direct relationship between the porosity formed by ice dendrites and the freezing rate. According to the results of Ghio *et al.* (12), who experimentally observed the same tendency as in our case, the porosity and permeability of the dry matrix increase the sublimation rate, which supports the notion that the slower the freezing rate is, the shorter will be the drying time. It has been reported that a slow cooling process and a high sublimation temperature provide the minimized freeze-drying processing time, as was noted by Choi *et al.* (13) in a study of the influence of freezing rate on the primary drying time for the freeze-drying of double emulsions. According to Tamman's theory, quick freezing causes the formation of small and numerous crystals, whereas slow freezing produces large and less numerous ice crystals (14). We represent this relationship in terms of ice crystal size and freeze-drying time in the following section.

**Ice dendrite size analysis** The examples in Fig. 6 show the crystal size distribution at 4 different positions at various cooling temperatures. Two means could be observed for all the experiments realized: the mean size of ice dendrite  $d_p$  and the width of the distribution increased with increasing distance from the copper plate.

Figure 7 demonstrated a linear relationship between the mean size of ice dendrites and the axial position at different cooling temperatures. As observed from the error bar ( $\pm 1$  standard deviation) in this figure, the variability in the observed mean ice dendrite size tended to increase with

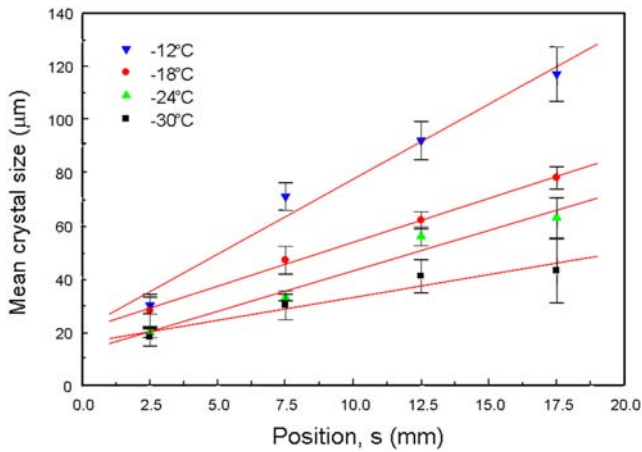


Fig. 7. Evolution of ice crystal size ( $d_p$ ) depending on the axial position.

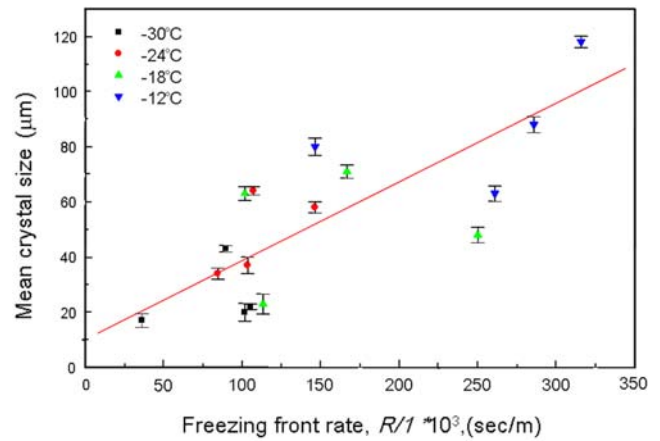


Fig. 8. Evolution of ice crystal size ( $d_p$ ) as a function of the inverse freezing front rate ( $1/R$ ) in tuna.

decreasing freezing rates in the same manner as was noted with the spread in the distribution of crystal size.

This can be attributed to the greater ice crystal size observed at lower freezing rates as compared to higher freezing rates. Therefore, at higher freezing rates the growth tends to be more homogenous and the variation in the mean size of ice dendrites is lower.

Finally, we can show the intergraded total value of the mean ice dendrite size depending on the freezing front rate, as is shown in Fig. 8. Then, we attempted to derive an empirical relationship from our experimental data, as follows:

$$d_p = a(1/R) + b \quad (4)$$

in which the  $a$  and  $b$  of the fitting parameters were  $2.85 \times 10^{-4}$  and  $10.1$  ( $r=0.89$ ), respectively. Thus, the mean size of the ice crystal dendrites was fitted as a function of the inverse freezing front rate,  $1/R$ . The ice dendrite size decreased with reductions in the freezing front rate; conversely, when the freezing rate was slower, the ice crystals were larger.

**Morphology analysis** We observed the morphology of the ice dendrites in the tuna samples via SEM, with a

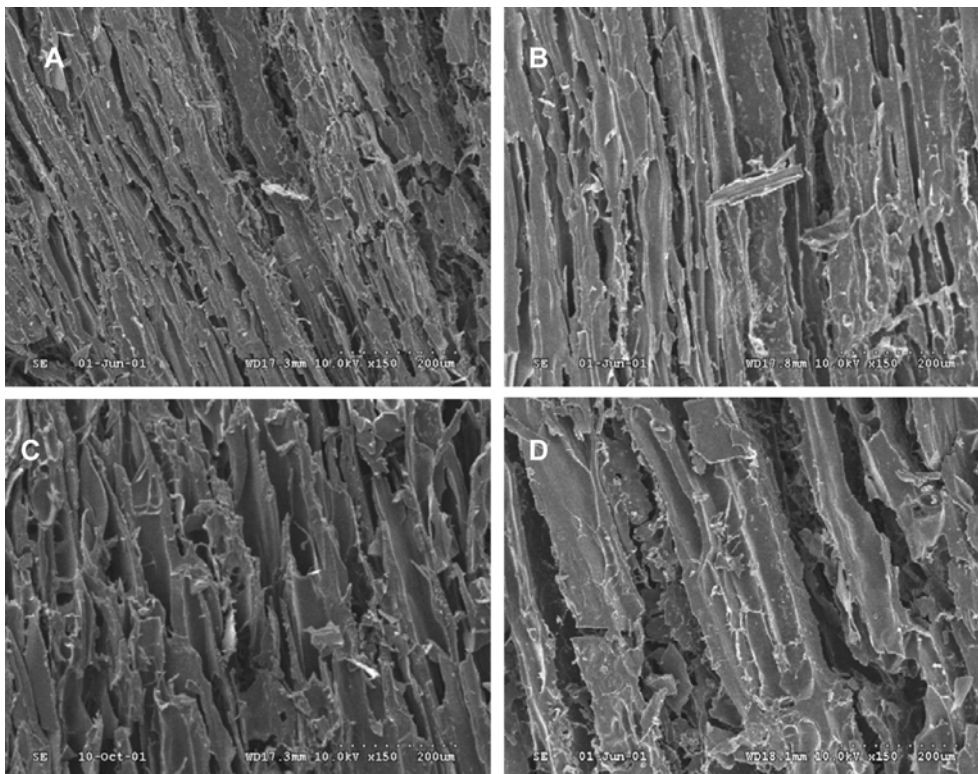


Fig. 9. Ice crystal size in vertical cross sections at 4 different positions from the bottom ( $T_c: -30^\circ\text{C}$ ). A, 2.5 mm; B, 7.5 mm; C, 12.5 mm; D, 17.5 mm.

**Table 3. Parameters of linear regression fit with  $a^* \cdot s + b^* = dp$  on the relationship between the axial position,  $s$  and the mean crystal size,  $dp$  and  $r$ , correlation coefficient**

Cooling temperature (°C)	$a^*$	$b^*$	$r$
-30	1.72	15.80	0.96
-24	3.04	12.60	0.98
-18	3.30	20.75	0.99
-12	5.64	21.10	0.98

variety of freezing rates. Figure 9 shows that the mean size of the ice dendrites increased as a function of the distance of the freezing front from the copper plate at the same cooling temperature. In addition, at the same position, the ice crystals were larger at higher cooling temperatures. Using the uni-directional heat transfer system, we validated the mathematical regression relationship from the measurements of the temperature transient fields and from the freezing front positions as a function of the freezing times.

Then, using this simplified mathematical relationship, we were able to derive the values of the main freezing process variables, such as the freezing front rate and the thermal gradient in the frozen zone at the interface. These values were employed to empirically correlate the mean size of the ice crystals, and our results showed that this characteristic size varied inversely with the freezing front rate (strong influence). Additionally, this mean size was globally proportional to the square root of the distance to the cooling plate.

Finally, we were able to compare the freeze-drying time in relation with the cooling temperature, namely, the freezing front rate. Our food device was a uni-directional heat transfer system for the formation of the ice crystal fingers, which meant that the ice channel operated as a route for the transformation from ice to vapor during freeze-drying. Thus, the ice crystal size affected the resistance to sublimation in the freeze-drying process. In general, small ice crystals are formed during a rapid freezing process. It has been empirically demonstrated that quick freezing results in the formation of small crystals, whereas slow freezing produces larger crystals. Several authors (8,15,16) have previously suggested the existence of a simple relationship between crystal size and operating conditions, but no complete theoretical analysis has yet been conducted in this regard.

## References

- Caillet A, Cogné C, Andrieu J, Laurent P, Rivoire A. Characterization of ice cream structure by direct optical microscopy influence of freezing parameters. *Lebensm. -Wiss. Technol.* 36: 743-749 (2003)
- Woinet B, Andrieu J, Laurent M. Experimental and theoretical study of model food freezing. Part I. Heat transfer modeling. *J. Food Eng.* 35: 381-393 (1998)
- Woinet B, Andrieu J, Laurent M, Min SG. Experimental and theoretical study of model food freezing. Part II: Characterization and modelling of the ice crystal size. *J. Food Eng.* 35: 395-407 (1998)
- Rahman MS, Sablandi SS. Structural characteristic of freeze-dried abalone. *T. I. Chem. Eng. -Lond.* 81: 309-315 (2003)
- Faydi E, Andrieu J, Laurent P. Experimental study and modelling of the ice crystal morphology of model standard ice cream. Part I: Direct characterization method and experimental data. *J. Food Eng.* 48: 283-291 (2001)
- Pardo JM, Suess F, Niranjana K. An investigation into the relationship between freezing rate and mean ice crystal size for coffee extracts. *T. I. Chem. Eng. -Lond.* 80: 176-182 (2002)
- Kurz W, Fisher DJ. Dendrite growth at the limit of stability: Tip radius and spacing. *Acta Metall. Mater.* 29: 11-17 (1981)
- Bomben JL, King CJ. Heat and mass transfer in the freezing of apple tissue. *J. Food Eng.* 17: 615-632 (1982)
- Kochs M, Körber CH, Heschel I, Nunner B. The influence of freezing process on vapour transport during sublimation in vacuum freeze-drying of macroscopic samples. *Int. J. Heat Mass Tran.* 36: 1727-1738 (1993)
- Kang CH, Jung HY, Lee DH, Park JK, Ha JU, Lee SC, Hwang YI. Analysis of chemical compounds on tuna processing by-products. *J. Korean Soc. Food Sci. Nutr.* 29: 981-986 (2000)
- Rahman MS, Kasapis S, Guizani N, Al-Amri OS. State diagram of tuna meat: Freezing curve and glass transition. *J. Food Eng.* 57: 321-326 (2003)
- Ghio S, Barresi AA, Rovero G. A comparison of evaporative and conventional freezing prior to freeze-drying of fruits and vegetables. *Food Bioprod. Process.* 78: 187-192 (2000)
- Choi MJ, Briançon S, Bazile D, Royere A, Min SG, Fessi H. Effect of cryoprotectant and freeze-drying process on the stability of W/O/W emulsions. *Dry. Technol.* 25: 809-819 (2007)
- Bevilacqua A, Zaritzky NE. Ice recrystallization in frozen beef. *J. Food Sci.* 47: 1410-1414 (1982)
- Bevilacqua A, Zaritzky NE, Calvelo A. Histological measurement in frozen beef. *J. Food Technol.* 14: 237-251 (1979)
- Miyawaki O, Abe T, Yano T. Freezing and ice structure formed in protein gels. *Biosci. Biotech. Bioch.* 56: 953-957 (1992)
- Min SG. Study on recrystallization of ice in frozen food. PhD thesis, University of Hohenheim, Germany (1994)